Available online at www.sciencedirect.com
ScienceDirect
Dyes and Pigments 79 (2008) 111–125
DYES and PIGMENTS
www.elsevier.com/locate/dyepig

Analysis of the photofading of phenylazo-aniline and phenylazo-pyridone disperse dyes on poly(ethylene terephthalate) substrate using the semiempirical molecular orbital PM5 method

Yasuyo Okada [a,*], Toshio Hihara [b], Zenzo Morita [c]

[a] School of Home Economics, Otsuma Women's University, Department of Life Design, Sanban-cho, Chiyoda-ku, Tokyo 102-8357, Japan
[b] Technical Center, DyStar Japan Ltd., Shinkai-machi 2-65, Omuta, Fukuoka-ken 836-0017, Japan
[c] Tokyo University of Agriculture and Technology, Koganei, Tokyo 184-8588, Japan

Received 29 November 2007; received in revised form 18 January 2008; accepted 19 January 2008
Available online 8 February 2008

Abstract

The photofading characteristics of six monoazo disperse dyes on polyester fabric upon exposure to a carbon arc in air were analyzed in terms of the reactivity (k_0) towards $^1O_2$ and the photosensitivity (f). The photochemical properties of the dyes were estimated by catalytic fading in mixture dyeings of two yellow (pyridone-azo and quinolone-azo) dyes. The k_0 ratios for the componential dyes in the 1:1 mixture dyeings varied with the partner yellow dye, implying that they depend upon the f values and the concentrations of the component dyes as well as the superposition of absorption spectra, and the changes in their concentration, even in the initial stages of fading. The relative k_0 values, as estimated by the sum of the electrophilic frontier densities using the PM5 method were demonstrated experimentally, while taking the influencing factors into consideration. The assumption that the rates of oxidative fading on PET were proportional to the product of two factors of k_0 and f was confirmed as reasonable based on the fading behavior upon exposure to a carbon arc in air of eight disperse azo dyes with a wide range of two factors.

Keywords: Disperse azo dye; Azo-hydrazone tautomerism; Photo-oxidation; Polyester fabric; PM5; Frontier orbital theory

1. Introduction

In a previous paper [1], the photofading profiles of pyridone-azo disperse dyes in the single and combination dyeings of poly(ethylene terephthalate) (PET) fabric upon exposure to a carbon arc in air were analyzed to elucidate the mechanism of oxidative fading. The fading characteristics of azo dyes in the single and combination dyeings can be explained in terms of two parameters: k_0, which is the second-order rate constant of the reaction with $^1O_2$ generated by the sensitization of dyes; and f, which is the quantum yield of the generation of $^1O_2$. The azo-hydrazone tautomerism (AHT) of reactive and disperse azo dyes in the gas and water phases was examined to identify the tautomers with high stability in cellulose and PET substrates, using the semiempirical molecular orbital (MO) PM5 method [1–5]. The reactivities, which were estimated as the k_0 values, for the tautomers on the substrates were correlated with the sum of the electrophilic frontier densities of the limited double bonds in the dye [5–8]. The photofading profiles of six disperse monoazo dyes on the PET and polyamide (nylon) substrates upon exposure of the dyed fabrics to a carbon arc were examined under various environmental conditions [9].

In the present paper, we analyzed the results of irradiation of monoazo disperse dyes on PET fabric by the same procedure as that of a previous paper [1]. The photosensitivity of six dyes and the ease with which the dye was photo-oxidized were experimentally determined utilizing the catalytic fading of yellow disperse dyes [1]. The k_0 values were also estimated by frontier orbital theory using the PM5 method [1,5–8]. The photochemical properties such as lightfastness (LF) and catalytic fading of six disperse azo dyes are discussed in terms of k_0 and f.

* Corresponding author. Tel.: +81 3 5275 5738; fax: +81 3 5275 7105.
E-mail address: yasuyo.okada@otsuma.ac.jp (Y. Okada).

0143-7208/$ - see front matter © 2008 Elsevier Ltd. All rights reserved.
doi:10.1016/j.dyepig.2008.01.013

2. Experimental

2.1. Dyes used

Six monoazo disperse dyes were used and two yellow pyridone-azo and quinolone-azo dyes were also used for the diagnostic test. The chemical structures of the azo (AT) or hydrazone (HT) tautomer of these dyes, which were determined to predominate on the PET substrate (cf. Section 3.2), together with the C.I. Generic Names, the C.I. Constitution Numbers (where available), and abbreviations (in parentheses), and the dominant tautomers are illustrated.

2.1.1. The six disperse phenylazo-pyridone and phenylazo-aniline dyes used

(1) C.I. Disperse Yellow 211, C.I. 12755, (Yellow 211), HT

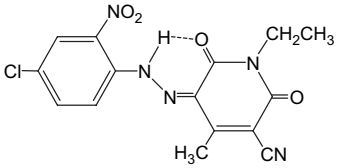

(2) C.I. Disperse Red 73, C.I. 11116, (Red 73), AT

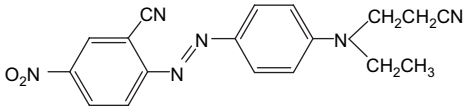

(3) C.I. Disperse Blue 79:1, C.I. 11344, (Blue 79:1), AT

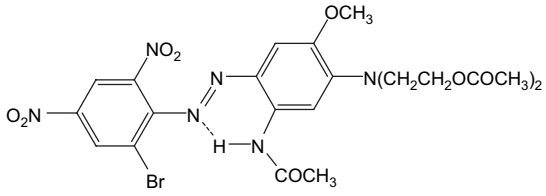

(4) C.I. Disperse Blue 165, C.I. 11077, (Blue 165), AT

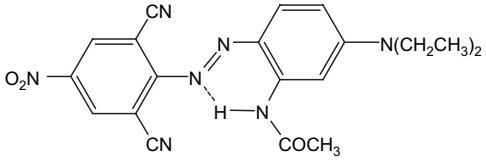

(5) C.I. Disperse Blue 291, C.I. 113395, (Blue 291), AT

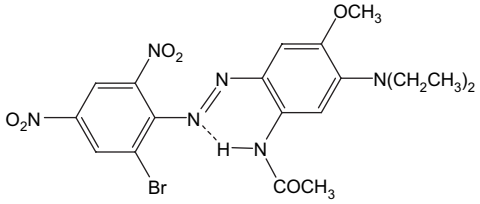

(6) A monoazo violet dye (Violet), AT

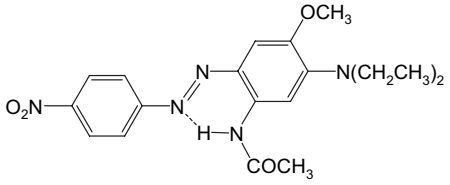

2.1.2. Yellow dyes for the diagnostic test

(1) C.I. Disperse Yellow 114, C.I. 128455 (Yellow 114), HT

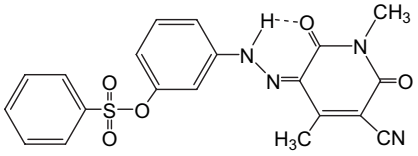

(2) A quinolone-azo dye (Quinolone), HTs

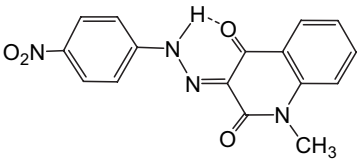

A-type of HT

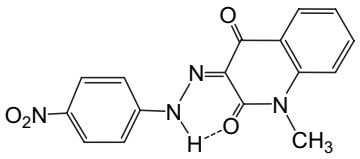

B-type of HT

The LF of these eight dyes, which are the same as those used previously [1,9] on the PET fabric are listed in Table 1.

2.1.3. Materials and methods for dyeing and exposure

The PET fabric used was double-pique grade F1142 (dtex/filament: 84/36, weight: 240 g/m^2; Toray Industries). The dyeing was carried out at 135 °C for 30 min at pH 4.5 using an acetic acid/sodium acetate buffer at a liquor ratio of 1:20 with six (yellow, red, violet and blue) azo dyes (*N*/3 depth) and two yellow dyes (*N*/2 depth), respectively, in both the single and combination dyeings. After dyeing, reduction clearing was performed at 80 °C for 15 min in a mixture of sodium hydroxide (2.0 g/dm^3), sodium dithionite (2.0 g/dm^3), and the nonionic surfactant, Sera Wash M-SF (1.0 g/dm^3; DyStar). Rinsing and drying were carried out after reduction clearing.

The dyed fabrics were exposed to a carbon arc using a fadeometer (Suga Test Instruments). The reflectance spectra of the dyed and exposed fabrics were measured using a V-550 UV–vis spectrophotometer equipped with an integrating sphere (Jasco Ltd).

Table 1
Analyses of photofading of aminoazobenzene dyes on PET fabric upon exposure to a carbon arc in air[a]

Dye	LF	Rate of fading from single dyeings (20–60 h)				k_0 by MO[e]	f	Order		Relative values
	$N/3$	Initial slope[b]	Relative values	Order[c]	Order of ΔE^*_{ab}	Relative values	Relative values	k_0 by MO	f	fk_0
Red 73	>6	0.415_7	1.00	1	1	1.00	1.00	1	1	1.00
Blue 165	6	0.596_6	1.44	2	2	1.17_6	1.22_0	3	2	1.43
Blue 79:1	4	1.07_5	2.59	3	3	2.01_7	1.28_1	4	3	2.58
Yellow 211	>6	1.14_4	2.75	4	5	1.02_2	2.69_2	2	6	2.75
Blue 291	3	2.01_8	4.85	5 (6)	3	2.48_8	1.94_5	7	5	4.84
Violet	2	4.52_8	10.89	6 (8)	8	3.19_4	3.41_0	8	7	10.9
Yellow 114	6-[d]	1.61_1	3.87	(5)	6	2.05_3	1.88_6	5	4	3.87
Quinolone	4–5[d]	3.45_0	8.30	(7)	7	2.18_0	3.80_6	6	8	8.30

[a] For order, larger number describes larger rates or values.
[b] Initial slope $= -\ln\{(\mathrm{KSR})_t/(\mathrm{KSR})_0\}/t$ ($\times 10^{-6}\,\mathrm{s}^{-1}$).
[c] The same order as that of relative values of fk_0. Order in parenthesis is the order when two yellow dyes were added.
[d] $N/2$ depth.
[e] cf. Fig. 1 through Tables 5 and 8 (see Section 3.3).

2.2. Molecular orbital calculations

All the MO calculations were carried out using CAChe MOPAC 2002 (Windows edition, version 6.1.12.33) (Fujitsu) [10]. For the ATs and HTs of the eight dyes in the gas and water phases, structure optimization was performed to derive the molecular parameters, which included the standard heat of formation [$\Delta_f H^0$ (gas) and $\Delta_f H^0$ (H_2O) (kcal mol^{-1}), in the gas and water phases, respectively], the energies of HOMO and LUMO (E_{HOMO} and E_{LUMO}, respectively), the electron densities in HOMO (d_{HOMO}), the electrophilic frontier densities ($f_r^{(E)}$), and the dipole moment (μ), in the gas phase, using the PM5 method. The COSMO method was used to calculate the parameters in the water phase. The $\Delta_f H^0$ (gas) values were also estimated for the reaction intermediates of the corresponding tautomers for the six dyes at the transition-state geometry (TSG). Structure optimization was carried out to calculate the $\Delta_f H^0$ (gas) values for the reaction intermediates and end products at the PM5 geometry.

3. Results and discussion

3.1. Estimation of photochemical properties of disperse dyes on PET

Photo-oxidative fading of disperse dyes occurs on the PET substrate under aerobic conditions. This was confirmed by the catalytic fading observed in the mixture dyeings with yellow and blue azo dyes, in that, catalytic fading can be attributed to the action of $^1O_2$ the generation of which is sensitized by effective $^1O_2$ sensitizers to accelerate the fading of the partner dye [11–16]. It is assumed as a first approximation that the reaction of the dye with $^1O_2$ on the PET substrate can be treated as a homogeneous system. With continuous irradiation, if a sufficient amount of oxygen is present in the substrate and supplied from the environment, the steady-state generation of $^1O_2$ in the mixture dyeings may be assumed as follows:

$$[^3O_2](f_{i\text{-Yellow}} + f_{\mathrm{Exam}})/2 < [^1O_2] < [^3O_2](f_{i\text{-Yellow}} + f_{\mathrm{Exam}}) \quad (1)$$

where $f_{i\text{-Yellow}}$ and f_{Exam} are the photosensitivities (−) for the ith yellow dye and the blue, violet or red disperse dyes, respectively, (the subscript ''Exam'' describes the dyes examined.) and the square brackets represent their concentrations (mol kg^{-1}). The left-hand side of Inequality (1) describes the limit of non-dependence of concentration, while the right-hand side shows the limit of complete dependence in the combination (1:1) dyeings. Since the absorption spectra for the two dyes on PET must overlap in the visible and UV regions, the effect of superposition may vary with the combination, dye concentrations and the concentration ratios in the original sample and exposed sample even in the initial period of exposure.

In the case of single dyeings, the sensitization of the ith dye is

$$[^1O_2] = [^3O_2]f_i \quad (2)$$

Since $[^1O_2]$ is kept constant during the initial period of irradiation, the reaction of the dye with $^1O_2$ may be regarded as being pseudo-first-order. When the second-order reaction occurs between the ith azo dye (D_i) and $^1O_2$ with assumed rate constant of $k_{0,i}$ (mol^{-1} kg s^{-1}), the equation for the second-order reaction is described in terms of the following steady-state approximation:

$$-\frac{\mathrm{d}[D_i]}{\mathrm{d}t} = k_{0,i}[^1O_2][D_i], \quad (3)$$

where t is the time of reaction.

In order to perform quantitative analysis, the Kubelka–Munk parameter, K/S, which is assumed to be proportional to the concentration, is calculated by

$$K/S = \frac{(1-R)^2}{2R} = \alpha C, \quad (4)$$

where R is the percentage reflectance divided by 100, C is the concentration of the dye on PET and α is the calibration factor or absorption coefficient, which varies with the dye and wavelength [17]. Since all the dyes are azo compounds with nearly similar absorption coefficients to each other, it is assumed that

α is constant in the range of concentrations examined. Therefore, the degrees of fading were treated as the ratios of the *K*/*S* values, since α may be cancelled by its ratio.

In the combination dyeings, the value of $[^1O_2]$ in Eqs. (1)–(3) is common to both the dyes on the substrate but varies with the dye combination (and usually with the concentrations, which are fixed according to the experimental conditions). Thus, from the *K*/*S* ratios of both the dyes at exposure of time t in the mixture dyeings, the ratios of $k_{0,\mathrm{Yellow}}/k_{0,\mathrm{Blue}}$ for the two dyes were obtained as follows:

$$\left(\ln\frac{[D_{t,i}]}{[D_{0,i}]}\right)_{t,\mathrm{Yellow}}\Big/\left(\ln\frac{[D_{t,i}]}{[D_{0,i}]}\right)_{t,\mathrm{Exam}}=\frac{k_{0,\mathrm{Yellow}}}{k_{0,\mathrm{Exam}}}, \tag{5}$$

where $[D_{0,i}]$ and $[D_{t,i}]$ are the initial concentration and the concentration after the exposure of time t for the ith dye, respectively. Using this equation, the ratios of $k_{0,\mathrm{Yellow}}/k_{0,\mathrm{Exam}}$ for the disperse dyes were determined by the fading of the mixture dyeings with six disperse dyes as the photosensitizer and two yellow dyes to be eaten.

On the other hand, in the case of single dyeings, since Eq. (3) is rewritten as follows:

$$\ln\frac{[D_{t,i}]}{[D_{0,i}]}=-k_{0,i}f_i[^3O_2]t. \tag{6}$$

The logarithmic *K*/*S* ratio of fading is proportional to the product of both the parameters.

The results for C.I. Disperse Yellow 211 and the $k_{0,\mathrm{Yellow}}/k_{0,\mathrm{Exam}}$ ratios for Quinolone, have been reported previously [1]. The solubility of oxygen in PET in air was estimated as 5.1×10^{-4} mol kg^{-1} at 25 °C [1,18]. This is not sufficiently high enough for dye oxidation, since the concentration of dyes in PET is of the order of 10^{-3} mol kg^{-1}. The amount of oxygen consumed by photo-oxidation is compensated by the amount attributed to adsorption on the surface and diffusion from the surface into the substrate.

3.2. Analysis of the photo-reactivity of yellow dyes by catalytic fading

The results for both the mixture dyeings of PET fabrics with the six disperse dyes examined and two yellow dyes (pyridone-azo and quinolone-azo dyes) and the single dyeings with each dye after exposure to a carbon arc in air are listed in Table 2. The CIE chromaticity parameters are listed as the differences between the original dyed fabrics and the samples exposed to the carbon arc for 40 h; the full fading behaviors are defined by the *K*/*S* values (Tables 3 and 4). Considerable differences in photofading were observed between the single and mixture dyeings, although the quantitative analyses of catalytic fading based on CIE chromaticity parameters were limited, as described in a previous paper [1].

The magnitude of fading for the single-dyed PET fabrics are not described by the values of ΔE^*_{ab} but by those of ΔL^*, Δa^* and Δb^*. The order of the rate of fading was (cf. Table 2):

$$\begin{aligned}\text{Violet} &> \text{Quinolone} \gg \text{Yellow 114} > \text{Yellow 211}\\ &> \text{Blue 79 : 1} \geq \text{Blue 291} > \text{Blue 165} > \text{Red 73}.\end{aligned} \tag{7}$$

The *K*/*S* values obtained by Eq. (4) or the original values, $(K/S)_{\mathrm{Orig}}$, at the $\lambda_{\max}$ of each dye in the mixture dyeings are listed in Table 3 for Quinolone and in Table 4 for Yellow 114, respectively.

Since there is little absorption of yellow dyes at the $\lambda_{\max}$ of blue and violet dyes and the absorption of blue dyes is weak at the $\lambda_{\max}$ of yellow dyes, the $(K/S)_{\mathrm{Orig}}$ values of the yellow dyes were reduced by the corresponding values attributable to overlapping. The reduced values of $K/S[(K/S)_{\mathrm{reduced}}]$ are also listed in the lower row of the corresponding dyes (Tables 3 and 4). In the case of Red 73 in combination with the yellow dye, the absorption spectra of the componential dyes overlapped each other at both $\lambda_{\max}$'s. In order to avoid the superposition of the absorption spectra, the absorption at 540 nm was used for Red 73, at which there was little absorption by the yellow dyes, while absorption at 390 nm was used for yellow dye, at which there was minimal absorption by Red 73. The overlap of the absorption spectra of Red 73 and the yellow dye was abrogated at the wavelengths listed above. From the *K*/*S* ratios, $(\mathrm{KSR})_{\mathrm{Red}}$, at the $\lambda_{\max}$ of individual dyes and the ratios of $k_{0,i}$ were obtained from Eq. (5) and are listed in Tables 3 and 4.

Applying Eq. (5) to the *K*/*S* ratios, the $k_{0,\mathrm{Yellow}}/k_{0,\mathrm{Exam}}$ values were obtained (Tables 3 and 4). Since the $k_{0,\mathrm{Yellow}}/k_{0,\mathrm{Exam}}$ values for the respective times of exposure exhibited some scattering, the averaged values are also listed.

Table 2
Photofading of PET fabrics dyed singly and in an admixture with monoazo dyes upon exposure to a carbon arc in air for 40 h, described by CIE chromaticity parameters

No	Dye 1	Dye 2	CIE parameters measured			
			ΔE^*_{ab}	ΔL^*	Δa^*	Δb^*
Photofading of mixture dyeings with dyes 1 and 2						
1	Quinolone	Blue 291	9.07	1.96	4.71	−7.45
2	Quinolone	Blue 79:1	9.44	2.08	3.80	−8.40
3	Quinolone	Violet	6.65	6.40	0.72	−1.65
4	Quinolone	Red 73	8.91	0.43	−0.59	−8.85
5	Quinolone	Blue 165	15.44	1.09	6.18	−14.10
6	Yellow 114	Blue 291	6.53	2.26	4.97	−3.57
7	Yellow 114	Blue 79:1	4.12	2.37	2.43	−2.32
8	Yellow 114	Violet	8.25	7.66	−0.17	3.06
9	Yellow 114	Red 73	3.72	1.06	−0.98	−3.43
10	Yellow 114	Blue 165	6.87	0.68	3.12	−6.09
No	Dye	KSR[a]	ΔE^*_{ab}	ΔL^*	Δa^*	Δb^*
Photofading of single dyeings						
1	Yellow 211	0.858	3.31	0.47	0.79	−3.32
2	Red 73	0.938	0.80	−0.41	−0.31	−0.46
3	Blue 79:1	0.820	2.71	2.08	−0.27	1.70
4	Blue 165	0.909	1.39	0.63	−0.17	1.22
5	Blue 291	0.758	2.68	2.20	0.89	1.24
6	Violet	0.512	11.99	7.95	−3.88	8.12
7	Quinolone	0.603	9.96	−0.65	1.10	−9.89
8	Yellow 114	0.816	5.34	−1.32	0.09	−5.12

[a] K/S ratio $=\mathrm{KSR}=(K/S)_t/(K/S)_0$.

Table 3
Reactivity ratios according to the Kubelka–Munk parameters for six dyes in mixture dyeings with Quinolone (cf. Table 1)

Dye (λ_{max})	Time of exposure	Mixture dyeing					$k_{0,Yellow}/k_{0,Exam}$[d] (order[b])		
		Quinolone (437 nm)			Dye examined				
		K/S_{Orig}	K/S_{Red}	KSR[a]	K/S	KSR[a]	Each exposure	Average	By MO
Red 73 (523 nm)	0	10.253							
	20	7.711							
	40	5.818							
	60	5.435							
	0	5.376[e]	4.918		6.212			6.2_1 (2)	2.2 (1)
	20	3.985	3.545	0.721	5.968	0.946	5.8_9		
	40	3.081	2.666	0.542	5.632	0.907	6.2_7		
	60	2.898	2.486	0.505	5.592	0.900	6.4_8		
	λ (nm)[c]	390			540				
Blue 79:1 (621 nm)	0	9.346	8.409		6.317			4.6_3 (3)	1.1 (3)
	20	7.235	6.348	0.755	5.975	0.946	5.09_8		
	40	5.068	4.271	0.508	5.374	0.851	4.19_7		
	60	4.578	3.790	0.451	5.311	0.841	4.59_8		
Blue 165 (629 nm)	0	9.032	8.569		9.989			8.6_2 (1)	1.9 (2)
	20	5.663	5.227	0.610	9.404	0.941	8.12_9		
	40	3.767	3.348	0.391	9.036	0.905	9.40_7		
	60	3.362	2.954	0.345	8.789	0.880	8.32_5		
Blue 291 (641 nm)	0	9.293	8.388		8.840			3.0_3 (4)	0.9 (4)
	20	6.836	6.006	0.716	8.101	0.916	3.80_7		
	40	5.227	4.506	0.537	7.035	0.796	2.72_5		
	60	4.241	3.574	0.426	6.514	0.717	2.56_4		
Violet (563 nm)	0	9.274			5.988			0.9_2 (5)	0.7 (5)
	20	7.063			4.576	0.764	0.82_8		
	40	5.060			3.569	0.596	0.95_8		
	60	4.313			3.166	0.529	0.98_8		
	0	5.408[e]	4.595						
	20	4.297	3.676	0.800					
	40	3.282	2.797	0.609					
	60	2.877	2.447	0.533					
	λ (nm)[c]	390							
Quinolone (437 nm)	0	8.193							
	20	6.050		0.738					
	40	4.943		0.603					
	60	3.939		0.481					

Dye	Time of exposure	Mixture dyeing					$k_{0,Yellow}/k_{0,Exam}$[d]		
		Yellow dye			Blue 165(629 nm)				
		K/S_{Orig}	K/S_{Red}	*KSR*	K/S	KSR	Each exposure	Average	By MO
Yellow 211 (451 nm)	0	8.450	8.006		10.160			2.4_6	0.9
	20	7.927	7.495	0.936	9.875	0.972	2.32_8		
	40	7.212	6.792	0.848	9.593	0.944	2.86_0		
	60	6.843	6.440	0.804	9.210	0.906	2.21_0		

[a] K/S ratio = KSR = $(K/S)_t/(K/S)_0$.
[b] Order of $k_{0,Exam}$. (The larger the number, the larger the values of $k_{0,Exam}$).
[c] Wavelength used to avoid the superposition of reflectance spectra.
[d] Experimental values were calculated by Eq. (5).
[e] The K/S values in the lower row for Red 73 and Violet are the corresponding $(K/S)_{Red}$ values.

The order of relative reactivity towards $^1O_2$ for the individual dyes, as determined in the combination dyeings with Quinolone, was as follows:

$$\text{Violet} > \text{Blue 291} > (\text{Yellow 211}) > \text{Blue 79 : 1} > \text{Red 73} > \text{Blue 165}. \quad (8)$$

The parentheses around Yellow 211 indicate that the data were taken from a previous paper [1], since no direct estimation was possible in the present study. (The $k_{0,Yellow}/k_{0,Exam}$ values observed for Yellow 211 was estimated to be 3.5_0 from the values of Blue 165 for two dyes.)

In the case of dyeings with Yellow 114, the order of relative reactivity was:

$$\text{Violet} > \text{Blue 291} > \text{Blue 79 : 1} > \text{Red 73} > \text{Blue 165}. \quad (9)$$

Table 4
Reactivity ratios according to the Kubelka–Munk parameters for six dyes in mixture dyeings with Yellow 114 (cf. Table 1)

Dye	Time of exposure	Mixture dyeings					$k_{0,Yellow}/k_{0,Exam}$[d] (Order[b])		
		Yellow 114 (433 nm)		Dye examined					
		K/S_{Orig}	K/S	KSR[a]	K/S	KSR[a]	Each exposure	Average	By MO
Red 73 (523 nm)	0	12.782			7.994				
	20	10.921			7.412				
	40	9.606			7.077				
	60	9.101			7.018				
	0	4.456[e]	3.932		7.050			3.6_2 (2)	2.1 (1)
	20	3.979	3.470	0.883	6.839	0.970	4.08_5		
	40	3.557	3.071	0.781	6.543	0.928	3.30_8		
	60	3.416	2.934	0.746	6.482	0.919	3.46_9		
	λ (nm)[c]	390			540				
Blue 79:1 (621 nm)	0	11.225	10.262		6.643			1.7_0 (3)	1.0 (3)
	20	9.667	8.790	0.857	6.052	0.911	1.65_5		
	40	7.969	7.188	0.700	5.387	0.811	1.70_2		
	60	7.485	6.730	0.656	5.210	0.784	1.73_2		
Blue 165 (629 nm)	0	11.008	10.519		10.263			7.6_9 (1)	1.7 (2)
	20	8.782	8.311	0.790	9.875	0.962	6.084		
	40	7.162	6.697	0.637	9.756	0.951	8.976		
	60	6.750	6.291	0.598	9.626	0.938	8.032		
Blue 291 (641 nm)	0	11.133	10.225		8.958			1.2_3 (4)	0.8 (4)
	20	8.921	8.169	0.799	7.412	0.827	1.18_1		
	40	7.437	6.780	0.663	6.482	0.724	1.27_2		
	60	6.860	6.248	0.611	6.031	0.673	1.24_4		
Violet (563 nm)	0	10.931			6.489			0.48_2 (5)	0.6 (5)
	20	8.519			4.457	0.687	0.417		
	40	6.783			3.417	0.527	0.502		
	60	6.064			3.002	0.463	0.529		
	0	4.636[e]	3.755						
	20	3.815	3.210	0.855					
	40	3.188	2.724	0.725					
	60	2.906	2.498	0.665					
	λ (nm)[c]	390							
Yellow 114 (433 nm)	0	10.087							
	20	8.849		0.877					
	40	8.227		0.816					
	60	7.140		0.708					

[a] K/S ratio = KSR = $(K/S)_t/(K/S)_0$.
[b] Order of $k_{0,Exam}$. (The larger the number, the larger the values of $k_{0,Exam}$).
[c] Wavelength used to avoid the superposition of reflectance spectra.
[d] Experimental values were calculated by Eq. (5).
[e] The K/S values in the lower row for Red 73 and Violet are the corresponding $(K/S)_{Red}$ values.

The order of reactivity for five dyes estimated by two yellow dyes was the same between the yellow dyes used. Possible reasons why the six disperse dyes exhibit this order of reactivity are discussed below.

3.3. Estimation of the reactivity of dyes towards $^1O_2$ using the PM5 method

The values of $\Delta_f H^0$ (gas) and $\Delta_f H^0$ (H_2O) for the ATs and HTs for the six dyes as well as the other parameters were estimated using the PM5 method, and the results are listed in Table 5. As indicated by the values of $\Delta_f H^0$ (gas) and $\Delta_f H^0$ (H_2O), Yellow 211 and the other yellow dyes (Yellow 114 and Quinolone [1]) exist as HTs in the gas and water phases as well as on PET fabric, while Red 73, Blue 79:1, Blue 165, Blue 291 and Violet exist as ATs. The d_{HOMO} at the main atomic positions for the predominant tautomers are shown in Table 6. The number of atomic positions is described at the bottom of Table 6.

3.3.1. Frontier electron density for electrophilic reaction towards $^1O_2$

Based on the frontier orbital theory, Fukui et al. [19–22] introduced a factor called the frontier electron density, $f_r^{(E)}$, for electrophilic-type reactions. Fukui's original expression can be written as follows:

$$f_r^{(E)} = \frac{\sum_{j=1}^{N} \nu_j \left(C_r^j\right)^2 \exp\left\{-\lambda\left(E_{HOMO} - E_j\right)\right\}}{\sum_{j=1}^{N} \nu_j \exp\left\{-\lambda\left(E_{HOMO} - E_j\right)\right\}}. \quad (10)$$

where N is the total number of orbitals, ν_j is the number of electrons in the jth orbital and is usually 0, 1, or 2, C_r^j is the

Table 5
The $\Delta_f H^0$ (gas) and $\Delta_f H^0$ (H_2O) (kcal mol^{-1}) values in the gas and aqueous phases, dipole moment, μ (debye), E_{HOMO} and E_{LUMO} values for the A and HTs of yellow azo dyes in the gas phase, and the $f_r^{(E)}$ value for the most probable tautomer, as estimated using the semiempirical MO PM5 method

	Yellow 211		Red 73	Blue 79:1		Blue 165		Blue 291		Violet	
M.W.	361.744		348.363	625.389		405.415		509.316		385.422	
	AT	HT	AT	AT	HT	AT	HT	AT	HT	AT	HT
$\Delta_f H^0$ (gas)	19.482	14.588	145.330	−152.082	−139.076	101.933	123.413	15.171	17.510	7.213	21.470
μ	6.216	9.080	7.336	4.679	6.157	5.121	7.904	6.454	6.395	5.622	8.122
E_{HOMO}	−9.372	−9.976	−9.017	−9.336	−9.223	−8.734	−9.158	−8.758	−8.682	−8.652	−8.715
E_{LUMO}	−2.217	−2.224	−1.964	−2.373	−2.327	−2.185	−2.391	−2.262	−2.277	−2.026	−2.008
$\Delta_f H^0$ (H_2O)	−0.058	−4.931	123.615	−186.613	−174.162	77.823	100.464	−9.194	−5.255	−15.790	0.481
$f_r^{(E)}$(site) for the most	HT		AT	AT		AT		AT		AT	
probable tautomer	0.267 (C1)		0.232 (C3)	0.149 (C1)		0.221 (C3)		0.272 (C1)		0.212 (C1)	
	0.101 (N7)		0.173 (C4)	0.215 (C2)		0.097 (C4)		0.042 (C2)		0.154 (C2)	
	0.288 (C5)		0.208 (C5)	0.069 (C3)		0.277 (C5)		0.170 (C3)		0.067 (C3)	
	0.088 (C6)			0.134 (C4)				0.106 (C4)		0.157 (C4)	
	0.045 (C14)			0.245 (C5)				0.235 (C5)		0.229 (C5)	
	0.076 (C9)			0.126 (C6)						0.064 (C6)	
			0.029 (C2)			0.029 (C2)					
			0.370 (C1)			0.394 (C1)		0.011 (C6)			
	0.038 (C10)		0.035 (C6)			0.016 (C6)				0.012 (N7)	
	0.022 (C11)		0.020 (N7)			0.003 (N7)				0.077 (N8)	
	0.069 (C12)		0.098 (N8)			0.122 (N8)					
	0.045 (C13)										
$S_{m,n}^{(E)}$	0.865		0.613	0.938		0.595		0.825		0.883	
$S_{m,n}^{\prime\prime(E)}$	0.249		0.245	0.346		0.268		0.378		0.413	

coefficient of the jth LCAO MO at the rth atomic position, E_j is the energy of the jth orbital, and λ is a scale factor that is usually set to 3.0 in these calculations [23]. In Eq. (10), aside from those electrons in the HOMO category, the contributions of electrons at the corresponding atomic sites in the MOs below the HOMO were taken into consideration, but the effects of LUMO energy for partner reactant molecules on the electrophilic reaction were not taken into consideration.

The electrophilic reactivity of the double bonds towards $^1O_2$ is described by the sum, $S_{m,n}^{(E)}$, of the $f_r^{(E)}$ values defined by Eq. (10) at the two adjacent atomic positions, as follows [5–8]:

$$S_{m,n}^{(E)} = \sum_{m,n} \{f_m^{(E)} + f_n^{(E)}\}, \tag{11}$$

where m and n denote the atomic positions of the corresponding double bonds. (For [4 + 2] cycloaddition, the atomic positions of the reaction were written as the double bonds as in the case of [2 + 2] cycloaddition.) When there was an overlap, the overlap position was counted only once, and double bonds with larger values of $(f_m^{(E)} + f_n^{(E)})$ were taken into consideration one by one.

For a series of reactive azo dyes such as pyrazolinylazo dyes, azobenzene dyes and azo dyes from γ-, J-, and H-acids, different close relationships between the logarithms of the experimental values of $k_{0,i}$ and the values of $S_{m,n}^{(E)}$ for dyes have been found which result in correlation lines of almost similar slope with different intercepts. This is due to the almost identical range of E_{HOMO} in each series of dyes [5–8].

In order to derive an equation for estimating chemical reactivity using perturbation theory, Fukui et al. [19] derived the other parameter of superdelocalizability as follows:

$$S^{(E)}(x) = 2\sum_{i}^{OCC} \frac{C_i(x)^2}{\alpha - E_i}(-\beta), \tag{12}$$

$$S^{(N)}(x) = 2\sum_{i}^{UNOCC} \frac{C_i(x)^2}{E_i - \alpha}(-\beta), \tag{13}$$

where $S^{(E)}(x)$ and $S^{(N)}(x)$ are the electrophilic and nucleophilic superdelocalizability at position x, respectively, α and β are the Coulomb and resonance integrals, respectively, given by the Hückel MO method for a planar-conjugated hydrocarbon molecule. The latter is multiplied so as to make it dimensionless. $C_i(x)$ denotes the coefficient of the ith orbital at position x and E_i is the energy (in eV) of the ith orbital. OCC and UNOCC indicate that the summation is made over all the occupied and unoccupied orbitals, respectively. Fukui et al. [19] have shown that $S^{(E)}(x)$ and $S^{(N)}(x)$ can be approximated by the contributions of HOMO and LUMO, respectively, as follows:

$$S'^{(E)}(x) \approx 2\frac{C_{HOMO}(x)^2}{\alpha - E_{HOMO}}(-\beta), \tag{14}$$

$$S'^{(N)}(x) \approx 2\frac{C_{LUMO}(x)^2}{E_{LUMO} - \alpha}(-\beta). \tag{15}$$

Some researchers have used similar equations to describe the reactivity of various molecules [24–28].

Stewart [10,23] has implemented these parameters to describe the relatively reactive positions in the frontier orbitals for the electrophilic, nucleophilic and radical reactions, respectively, as electrophilic, nucleophilic and radical susceptibilities [frontier electron density for an electrophilic reaction is given by Eq. (10)], and to describe the relative magnitudes

Table 6
The d_{HOMO}, for phenylazo-aniline and phenylazo-pyridone disperse dyes

	Red 73[a]	Blue 79:1[b]	Blue 165[c]	Blue 291[d]	Violet[e]		Yellow 211[f]
	AT	AT	AT	AT	AT		HT
C1	0.192	0.100	0.213	0.142	0.123	C1	0.178
C2	0.011	0.164	0.005	0.016	0.077	C2	0.002
C3	0.119	0.020	0.101	0.083	0.014	N3	0.004
C4	0.091	0.079	0.053	0.056	0.090	C4	0.000
C5	0.105	0.118	0.142	0.120	0.129	C5	0.186
C6	0.014	0.074	0.003	0.000	0.019	C6	0.051
N7	0.006	0.000	0.000	0.000	0.000	N7	0.058
N8	0.044	0.030	0.064	0.038	0.039	N8	0.267
C9	0.002	0.000	0.000	0.000	0.002	C9	0.022
C10	0.000	0.002	0.002	0.001	0.005	C10	0.013
C11	0.000	0.000	0.000	0.000	0.000	C11	0.002
C12	0.000	0.000	0.000	0.002	0.006	C12	0.017
C13	0.000	0.000	0.000	0.000	0.000	C13	0.009
C14	0.002	0.005	0.002	0.001	0.006	C14	0.021
N15	0.000	0.000	0.000	0.000	0.000	N15	0.000
O16	0.000	0.000	0.000	0.000	0.000	O16	0.002
O17	0.000	0.000	0.000	0.000	0.000	O17	0.001
C(18)	0.000	0.000				Cl (18)	0.011
N19	0.311	0.018	0.320	0.382	0.233		

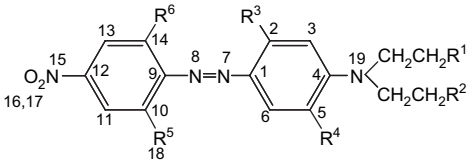

[a] Red 73, $R^1 = R^5 = CN$, $R^2 = R^3 = R^4 = R^6 = H$.
[b] Blue 79:1, $R^1 = R^2 = OCOCH_3$, $R^3 = NHCOCH_3$, $R^4 = OCH_3$, $R^5 = NO_2$, $R^6 = Br$.
[c] Blue 165, $R^1 = R^2 = R^4 = H$, $R^3 = NHCOCH_3$, $R^5 = R^6 = CN$.
[d] Blue 291, $R^1 = R^2 = H$, $R^3 = NHCOCH_3$, $R^4 = OCH_3$, $R^5 = NO_2$, $R^6 = Br$.
[e] Violet, $R^1 = R^2 = R^5 = R^6 = H$, $R^3 = NHCOCH_3$, $R^4 = OCH_3$.
[f] Yellow 211, as set.

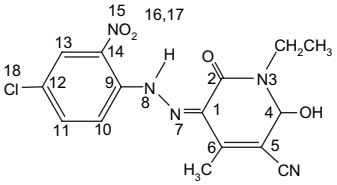

of overlap or delocalization energy between the two frontier MOs of the reagents, respectively, as electrophilic, nucleophilic and radical superdelocalizabilities using MOPAC software. The latter superdelocalizabilities, $S^{(E)}(x)$ and $S^{(N)}(x)$, on the other hand, are given as follows:

$$S^{(E)}(x) = \sum_{i=1}^{HOMO} \frac{2C_i(x)^2}{E^{E}_{LUMO} - E_i}(-\beta), \tag{16}$$

$$S^{(N)}(x) = \sum_{i=1}^{LUMO} \frac{2C_i(x)^2}{E_i - E^{N}_{HOMO}}(-\beta). \tag{17}$$

The choice of reagent energies, E^{E}_{LUMO} [LUMO energy of electrophile, α in Eq. (14)] and E^{N}_{HOMO} [HOMO energy of the nuceophile, α in Eq. (15)], is crucial to the successful application of superdelocalizability, especially when comparing the reactivity against different reagents [10,23].

In the present paper, taking into consideration only the effect of the orbital energy differences between the dye and $^1O_2$ in the denominator of Eq. (16), the electrophilic superdelocalizability may be approximated as the first approximation from Eqs. (10) and (16) as follows:

$$S''^{(E)}_{m,n} = \frac{S^{(E)}_{m,n}(-\beta)}{E^{^1O_2}_{LUMO} - E^{Dye}_{HOMO}}, \tag{18}$$

where β is multiplied to make it dimensionless (−1.0 eV). The contribution of electrons to the reactivity in the orbitals with lower energies than the HOMO in the dye molecule is taken into consideration in Eq. (10), while the contribution of the orbital energy difference between the dye and $^1O_2$ is taken into consideration only by the denominator of Eq. (18). In the present paper, all the double bonds which possess possible reactivity towards $^1O_2$ are described as potential double bonds. The limited double bonds exhibiting reactivity actually towards $^1O_2$ among the potential double bonds are described theoretically by $S^{(E)}_{m,n}$ (Eq. (11)) or more generally by $S''^{(E)}_{m,n}$ (Eq. (18)). The validity has been experimentally confirmed in a series of papers [5–8].

3.3.2. Reactivity towards $^1O_2$ for the ATs of Blue 165 in terms of $f_r^{(E)}$

$^1O_2$ adds to the double bonds in aromatic molecules *via* the ene reaction and [2 + 2] cycloaddition (hereafter, 'addition' is used for 'cycloaddition'). The potential double bonds in the ATs of Blue 165 to which $^1O_2$ can add are C1=C2, C2=C3, C3=C4, C4=C5, C5=C6, C1=C6 and N7=N8. The $\Delta_f H^0$ (gas) values of reaction intermediates from the potential double bonds at the TSG and optimized geometry (derived by the PM5 method), as well as those for the reaction products are listed in Table 7. For the six dyes examined, there were only small differences in the $\Delta_f H^0$ (gas) values for the intermediates of the reaction with $^1O_2$ at the TSG among the potential reaction modes at the possible reaction sites with few exceptions as in the cases of reactive dyes [5–8]. However, since there were considerable differences in the $\Delta_f H^0$ (gas) values for the reaction products, the order of reactivity for the potential reaction modes was compared based on these values (cf. Section 3.3.5). From the $\Delta_f H^0$ (gas) values for the reaction products, the order of reactivity for the potential double bonds was as follows:

$$\begin{aligned} \text{ene(C3=C2;H(N20))} &> [2+2]\text{addition(C5=C6)} \\ &\approx [2+2]\text{addition(C3=C2)} \\ &> [2+2]\text{addition(C6=C1)} \\ &> [2+2]\text{addition(C4=C5)} \\ &> [2+2]\text{addition(C3=C4)} \\ &> [2+2]\text{addition(N7=N8).} \end{aligned} \tag{19}$$

The $f_r^{(E)}$ values of the sites corresponded to the potential double bonds are listed in Table 5. Although the order of reactivity derived from the $f_r^{(E)}$ values was different from that

Table 7
The $\Delta_f H^0$ (gas) (kcal mol^{-1}) of intermediate and end products in the ene and [2 + 2] cycloaddition reactions at the double bonds of C1═C2, C2═C3, C3═C4, C5═C6, C1═C6 etc. for the HTs of Yellow 211 and the ATs of aminoazobenzene dyes with singlet oxygen

Dye	Tautomer	$\Delta_f H^0$ (gas) of intermediate at TSG	$\Delta_f H^0$ (gas) of intermediate	$\Delta_f H^0$ (gas) of hydroperoxide	$\Delta_f H^0$ (gas) of intermediate at TSG	$\Delta_f H^0$ (gas) of intermediate	$\Delta_f H^0$ (gas) of addition product
Mode (position)		Ene (C1═N7; H(N8))			[2 + 2] Addition (C1═N7)		
Yellow 211	HT	38.972	39.012	1.605	38.979	38.985	34.481
Mode (position)		Ene (C1═C2; H(N20))			[2 + 2] Addition (C1═C2)		
Yellow 211	HT	–	–	–	39.073	39.083	11.544
Red 73	AT	–	–	–	174.665	174.676	158.471
Blue 79:1	AT	−129.452	−129.418	−155.198	−129.452	−129.446	−150.347
Blue 165	AT	132.242	132.243	113.136	147.137	147.272	114.183
Mode (position)		Ene (C3═C2; H(N20))			[2 + 2] Addition (C3═C2)		
Red 73	AT	–	–	–	175.543	175.544	155.451
Blue 79:1	AT	−128.469	−128.459	−157.990	−128.394	−128.393	−151.154
Blue 165	AT	132.299	132.334	103.864	147.007	147.019	108.502
Mode (position)		Ene (C10═C9; H(N8))			[2 + 2] Addition (C10═C9)		
Yellow 211	HT	39.010	39.170	−1.377	39.016	39.139	20.477
Mode (position)		Ene (C14═C9; H(N8))			[2 + 2] Addition (C14═C9)		
Yellow 211	HT	39.030	39.042	1.568	39.049	39.106	21.100

Dye	Tautomer	$\Delta_f H^0$ (gas) of intermediate at TSG	$\Delta_f H^0$ (gas) of intermediate	$\Delta_f H^0$ (gas) of addition product	$\Delta_f H^0$ (gas) of intermediate at TSG	$\Delta_f H^0$ (gas) of intermediate	$\Delta_f H^0$ (gas) of addition product
Mode (position)		[2 + 2] Addition (C3═C4)			[2 + 2] Addition (C5═C6)		
Yellow 211	HT	–	–	–	39.016	39.045	21.360
Red 73	AT	174.688	174.704	155.545	175.327	175.344	156.212
Blue 79:1	AT	−128.338	−128.253	−149.966	−128.533	−128.526	−157.828
Blue 165	AT	134.122	134.126	119.560	134.875	135.002	108.030
Mode (position)		[2 + 2] Addition (N7═N8)			[2 + 2] Addition (C4═C5)		
Red 73	AT	174.887	174.946	192.645	175.402	175.406	156.532
Blue 79:1	AT	−129.605	−129.590	−131.625	−128.506	−128.490	−153.945
Blue 165	AT	134.111	134.200	134.200	134.026	134.055	118.598
Mode (position)		[2 + 2] Addition (C6═C1)					
Red 73	AT	175.235	175.235	158.234			
Blue 165	AT	147.210	147.240	117.125			
Mode (position)		[2 + 2] Addition (C11═C12)			[2 + 2] Addition (C13═C14)		
Yellow 211	HT	39.078	39.100	22.363	396.016	39.045	21.360
Mode (position)	[4 + 2] Addition (C1═C4)						
Yellow 211	HT	39.061	39.076	9.865			

derived from the $\Delta_f H^0$ (gas) values, the reactivity of double bonds: C1═C2, C2═C3, C5═C6, C6═C1 and N7═N8 were excluded due to the low values of d_{HOMO} at C2 (0.005), C6 (0.003) and N7 (0.000) (Table 6), which were demonstrated also by the $f_r^{(E)}$ values listed in Table 5. The double bonds in the diazo component were excluded due to the alternate distribution of d_{HOMO} and $f_r^{(E)}$. As a result, only two of the double bonds: C3═C4 and C4═C5 in Blue 165 had reactivity towards $^1O_2$ as shown by the $S_{m,n}^{(E)}$ values listed in Table 5, resulting in the next lowest reactivity among the six dyes examined.

3.3.3. Reactivity towards $^1O_2$ for the ATs of Red 73 in terms of $f_r^{(E)}$

The potential double bonds in the ATs of Red 73 to which $^1O_2$ can add are C1═C2, C2═C3, C3═C4, C4═C5, C5═C6, C1═C6 and N7═N8. From the $\Delta_f H^0$ (gas) values for the reaction products, the order of reactivity for the potential double bonds was as follows:

$$\begin{aligned}&[2+2]\text{addition(C2═C3)} \approx [2+2]\text{addition(C3═C4)}\\ &> [2+2]\text{addition(C5═C6)} \approx [2+2]\text{addition(C4═C5)}\\ &> [2+2]\text{addition(C1═C6)} \approx [2+2]\text{addition(C1═C2)}\\ &\gg [2+2]\text{addition(N7═N8)}.\end{aligned} \quad (20)$$

The $f_r^{(E)}$ values for the potential double bonds are listed in Table 5. Although the order of reactivity derived from the $f_r^{(E)}$ values of the double bonds was different from that derived from the $\Delta_f H^0$ (gas) values, the reactivity of double bonds: C1═C2, C2═C3, C5═C6, C6═C1 and N7═N8 were excluded due to the low values of d_{HOMO} at C2 (0.011), C6 (0.014) and N7 (0.006) (Table 6), which are demonstrated also by the $f_r^{(E)}$ values listed in Table 5 as in the case of

Blue 165. Since the $\Delta_f H^0$ (gas) value of the reaction products for [2 + 2] addition (N7═N8) was considerably higher than that of the reaction intermediate (Table 7), this reaction mode, if it occurs at all, may terminate at the intermediate product. All the double bonds in the diazo component were excluded due to the completely alternate distribution of d_{HOMO} and $f_r^{(E)}$. This dye possesses only two double bonds exhibiting reactivity towards $^1O_2$ and resulted in lower reactivity than Blue 165.

Applying the same procedure to the ATs of Blue 291 and Violet, the reactivity towards $^1O_2$ was examined and summarized in Table 5 (cf. Table 6). From the $S_{m,n}^{(E)}$ values for the limited double bonds, the order of reactivity for the four dyes examined above was:

$$\text{Violet} > \text{Blue 291} \gg \text{Red 73} > \text{Blue 165}. \quad (21)$$

As far as these four dyes are concerned, this order which was estimated based on the $S_{m,n}^{(E)}$ values in Table 5 using the PM5 method coincides with the order determined experimentally [cf. Inequality (8) and (9)].

3.3.4. Reactivity towards $^1O_2$ for the ATs of Blue 79:1 in terms of $f_r^{(E)}$

From the $\Delta_f H^0$ (gas) values for the reaction products, the order of reactivity for potential double bonds in the ATs of Blue 79:1 is as follows:

$$\begin{aligned}&\text{ene(C3═C2; H(N20))} \approx [2+2]\text{addition(C5═C6)}\\ &> \text{ene(C1═C2; H(N20))} > [2+2]\text{addition(C4═C5)}\\ &> [2+2]\text{addition(C3═C2)}\\ &\approx [2+2]\text{addition(C1═C2)} \approx [2+2]\text{addition(C3═C4)}\\ &> [2+2]\text{addition(N7═N8)}. \end{aligned} \quad (22)$$

There are no d_{HOMO} values that contribute to the reactivity in the diazo component. The order of reactivity derived from the $f_r^{(E)}$ values of the double bonds was different from that derived from the $\Delta_f H^0$ (gas) values. The ene reactions occurred more easily than the corresponding [2 + 2] addition reactions did at the same double bonds (Table 7). As in the case of Red 73, the reaction mode of [2 + 2] addition (N7═N8) may be excluded from the reactivity. All the double bonds in the coupling component (benzene ring) possess reactivity towards $^1O_2$ as in the case of Violet, although the reactivity $(S_{m,n}^{(E)})$ derived from the sum of $f_r^{(E)}$ for the double bonds exhibiting reactivity of Violet was smaller than that of Blue 79:1 (Table 5), which was opposite of the result obtained by experimentation. This discrepancy is discussed below, together with issues relating to Yellow 211.

3.3.5. Reactivity towards $^1O_2$ for the HTs of Yellow 211 in terms of $f_r^{(E)}$

From the $\Delta_f H^0$ (gas) values for the reaction products (Table 7), the order of reactivity for potential double bonds in the HTs of Yellow 211 is as follows [1]:

$$\begin{aligned}&\text{ene(C10═C9; H(N8))} > \text{ene(C14═C9; H(N8))}\\ &\approx \text{ene(C1═N7; H(N8))} \gg [4+2]\text{addition(C1═C4)}\\ &\gg [2+2]\text{addition(C10═C9)}\\ &\approx [2+2]\text{addition(C14═C9)} \approx [2+2]\text{addition(C5═C6)}\\ &= [2+2]\text{addition(C13═C14)}\\ &> [2+2]\text{addition(C11═C12)}\\ &\gg [2+2]\text{addition(C1═N7)}. \end{aligned} \quad (23)$$

The order of reactivity derived from the $f_r^{(E)}$ values for the potential double bonds was different from that derived from the $\Delta_f H^0$ (gas) values. All the double bonds in the diazo component were excluded due to the completely alternate distribution of $f_r^{(E)}$ and the low values of d_{HOMO} at C10 (0.013), C11 (0.002) and C13 (0.009), with the exception of the double bond of C14═C9 (Table 6). The [4 + 2] addition (C1═C4) may be excluded due to the low value of d_{HOMO} at C4 (0.000). Based on $S_{m,n}^{(E)}$ values, this dye has relatively low reactivity towards $^1O_2$ among the six dyes examined, which supports the experimental observations of reactivity.

In the present reactivity analysis using the PM5 method, the $f_r^{(E)}$ and $S_{m,n}^{(E)}$ values exhibited the site dependence within the potential double bonds, although $S_{m,n}^{(E)}$ showed a close relationship with the reactivity towards $^1O_2$, as mentioned below. The $\Delta_f H^0$ (gas) values of the reaction intermediates at TSG and PM5 geometry exhibited no or small site dependence, although those of reaction products showed site dependence. These tendency may indicate that the $S_{m,n}^{(E)}$ values exhibit the reactivity of molecules with original geometry before the reaction started and that $\Delta_f H^0$ (gas) values correspond to the TSG after the molecular arrangement occurred. Thus, the reactivity towards $^1O_2$ of dyes can be expressed by the $S_{m,n}^{(E)}$ values. The $\Delta_f H^0$ (gas) values of the intermediates may show no site dependence since the double bonds possess potentially the same reactivity when the addition of $^1O_2$ occurred accompanying with molecular arreangement. The energy difference between reactants and products whose $\Delta_f H^0$ (gas) values are listed in Table 7, corresponds to the standard enthalpy of reaction. The lower the $\Delta_f H^0$ (gas) values for the products, which were used as the second criterion of reactivity in this paper, the more the reaction at the sites is exothermic. These tendencies are common with the cases of reactive dyes [5–8].

3.3.6. Extension of the present analyses to two yellow azo dyes

Taking into consideration the previous paper [1], quinolone-azo and pyridone-azo dyes, the fading behaviors of which were examined in the combination dyeings with six disperse azo dyes, are discussed in the context of the analyses of the present dyes using the PM5 method. The essential results from the MO calculations are listed as the relative values of $k_{0,i}$ in Table 1. From the $S_{m,n}^{\prime\prime(E)}$ values, which were estimated by the frontier orbital theory using the PM5 method, Yellow 114 and Quinolone possess almost identical $k_{0,i}$ values [1]. Yellow 114 may exist predominantly as HTs, while Quinolone exists as a 1:1 mixture of both the HTs of A-type and B-type tautomers (described in Section 2.1.2). But since the sum of

$f_r^{(E)}$ for both the HTs of A-type and B-type tautomers are almost identical with each other, only the HTs of B-type were taken into consideration. Since Yellow 114 and Quinolone possess relatively large $k_{0,i}$ values among the eight dyes listed in Table 1, their LF is moderate and they have relatively high sensitivity to catalytic fading. If the two bottom lines in Table 1 are added, the present analyses can be easily extended to both the yellow dyes, which in turn indicate the validity of the present analysis. (The order of the rate of fading together with two yellow dyes is listed in parentheses in Table 1.)

3.3.7. Relationship between k_0 and $S''^{(E)}_{m,n}$ values for the dominant tautomers of the yellow azo dyes

In a series of reactive monoazo dyes derived from the common coupling components, it has been reported that reactivity of these dyes towards $^1O_2$ described by the $S^{(E)}_{m,n}$ values are closely correlated with the log k_0 values determined experimentally [5–8]. This has been attributed to the narrow range of E_{HOMO} values in each series of dyes. Thus, in monoazo reactive dyes the substituents in diazo component act to shift only electrons, while those in the *N*,*N*-disubstituted azobenzenes act to shift both electrons and MO energies. According to frontier orbital theory, stabilization energies generated by the electrophile–nucleophile interactions in conjugated molecules are derived by perturbation analysis [19–22] and are described by the electron densities of HOMO (of the dye) and LUMO (of $^1O_2$) at the interacting sites in the conjugated two molecules (the product of the coefficients of the MOs) and the energy difference between HOMO (of dye) and LUMO (of $^1O_2$) as shown in Eq. (18).

Adding Blue 79:1 and Yellow 211 to the four dyes in Inequality (21) mentioned above (cf. Sections 3.3.2–3.3.5), the order of reactivity derived from the $S^{(E)}_{m,n}$ values (Table 5) becomes:

$$\text{Blue } 79:1 > \text{Violet} > \text{Yellow 211} > \text{Blue 291} \gg \text{Red 73} > \text{Blue 165}. \quad (24)$$

The E_{HOMO} values range from −10 eV (HT of Yellow 211) to −8.7 eV (AT of Violet), which is relatively narrow range compared to those seen for each series of reactive monoazo dyes.

Taking into consideration the effect of orbital energy differences between the HOMO of the dyes and the LUMO of $^1O_2$, and assuming that E_{LUMO} for $^1O_2$ is −6.51 eV [3], the order of reactivity derived from the $S''^{(E)}_{m,n}$ values (listed in the bottom lines of Tables 5 and 8) becomes:

$$\text{Violet} > \text{Blue 291} > \text{Blue } 79:1 > \text{Blue 165} > \text{Yellow 211} \approx \text{Red 73}. \quad (25)$$

This is almost identical to the order of experimental results expressed by Inequality (8) and (9). When the two yellow dyes were added, the order of reactivity [Inequality (25)] becomes (Table 1):

Table 8
The $\Delta_f H^0$ (gas) and $\Delta_f H^0$ (H_2O) (kcal mol^{-1}) values in the gas and aqueous phases, dipole moment, μ (debye), E_{HOMO} and E_{LUMO} values for the A and HTs of Yellow 114 and Quinolone in the gas phase, and the $f_r^{(E)}$ value for the most probable tautomer, as estimated using the semiempirical MO PM5 method

	Yellow 114		Quinolone			
M.W.	424.430		324.295			
	AT	HT	AT (A-type)	HT (A-type)	AT (B-type)	HT (B-type)
$\Delta_f H^0$ (gas)	−55.961	−63.007	21.209	15.096	17.556	15.005
μ	7.768	8.664	10.502	9.718	8.964	9.329
E_{HOMO}	−9.057	−9.307	−9.236	−9.377	−9.407	−9.325
E_{LUMO}	−1.779	−1.986	−2.089	−1.930	−1.754	−1.982
$\Delta_f H^0$ (H_2O)	−84.717	−93.521	0.575	−5.889	−4.494	−6.536
$f_r^{(E)}$(position)	HT		HT		HT	
for the most	0.139 (C14)		0.051 (C7)		0.050 (C7)	
probable	0.124 (C9)		0.181 (C8)		0.181 (C8)	
tautomer	0.102 (C10)		0.123 (C10)		0.124 (C10)	
	0.063 (C11)		0.107 (C4)		0.104 (C4)	
	0.166 (C12)		0.105 (C3)		0.101 (C3)	
	0.344 (C1)		0.099(C18)		0.098 (C18)	
	0.035 (N7)		0.074(C13)		0.067 (C13)	
	0.213 (C5)		0.086 (C14)		0.087 (C14)	
	0.030 (C6)		0.180 (C1)		0.199 (C1)	
	0.037 (C13)		0.025 (C9)		0.024 (C9)	
			0.014 (N11)		0.010 (N11)	
$S^{(E)}_{m,n}$	0.973		1.006		1.011	
$S''^{(E)}_{m,n}$	0.348		0.351		0.359	

$$\text{Violet} > \text{Blue 291} > \text{Quinolone} > \text{Yellow 114} \approx \text{Blue } 79:1 \gg \text{Blue 165} > \text{Yellow 211} > \text{Red 73}. \quad (26)$$

The substituents in the disperse azo dyes act to shift electrons as well as the orbital energies and affect the probability of internal conversion and intersystem crossing. Using frontier orbital theory, these phenomena are discussed in semi-quantitative terms below.

3.4. Estimation of performance parameters: $k_{0,i}$ and f_i from experiments

3.4.1. Values of $k_{0,i}$ obtained from combination dyeings

According to the simplest analysis of photofading in the disperse dye–PET system (cf. Section 3.1), combining Eqs. (1) and (3) gives a relationship between the left-hand-side of Eq. (6) and t with a slope proportional to $f_i k_{0,i}$, from which the relative values of f_i can be obtained from the ratios of $k_{0,Yellow}/k_{0,Blue}$. Based on the results of a previous study [1], two yellow dyes, Quinolone and Yellow 114, were selected as the diagnostic agents to estimate the potential properties of the dyes. From the combination dyeings with the two yellow dyes, the ratios of the relative fading or the slope, $\ln\{(KSR)_t/(KSR)_0\}/t$ for the componential dyes as well as the values of $k_{0,Yellow}/k_{0,Exam}$ are listed in Tables 3 and 4. If the ratios of the values of $k_{0,Yellow}/k_{0,Exam}$ for each of Quinolone and Yellow 114 are nearly constant, the assumption

made in the derivation holds. According to frontier orbital theory using the PM5 method, the $k_{0,i}$ values for the two yellow dyes were almost identical. Although this was not the case, the orders of the $k_{0,\mathrm{Yellow}}/k_{0,\mathrm{Exam}}$ values were similar, as summarized in Tables 3 and 4. As predicted from the observed phenomena, the values of $k_{0,\mathrm{Yellow}}/k_{0,\mathrm{Exam}}$ obtained exhibit dependence on the dyes in each combination and their photosensitivities. In addition to the sum of the photosensitivities of the componential dyes, photosensitivity was influenced by the inevitable superposition of absorption spectra for the two dyes over the whole range of the UV–vis region, even if the same yellow dye was used as the diagnostic agent. The total f_i values may decrease as the superposition of absorption spectra increases. However, since the absorption band with smaller wavelength than the $\lambda_{\max}$ was generated by the superposition of multiple transitions (the assignments of which are unknown), no quantitative analysis was possible. Paying little attention to the detailed dependence upon the combinations, the orders of the apparent $k_{0,i}$ values for the two yellow dyes are summarized in Tables 3 and 4. The order of the $k_{0,i}$ estimated experimentally is as follows:

$$\text{Violet} > \text{Blue 291} > \text{Blue 79 : 1} > \text{Red 73} > \text{Blue 165}. \tag{27}$$

The validity of this order is discussed comparing it with the order (25) derived by the MO method (cf. Section 3.3.7).

3.4.2. Estimation of f_i from single dyeings

From the plots of ln $k_{0,i}$ against $S''^{(\mathrm{E})}_{m,n}$ (cf. Fig. 1; if in order to plot this relationship, a hypothetical value of $k_{0,i}$ is inserted, the values for the other dyes can be determined. Thus, the ordinate of Fig. 1 is described as the optional scale.), the relative values of $k_{0,i}$ thus determined for each dye are listed in Table 1, with the assumption that the relative value of Red 73 is assigned a value of 1.0 as the reference.

On the other hand, the fading profiles for the six dyes examined and the two yellow dyes on PET fabric on exposure to a carbon arc in air are illustrated in Fig. 2. The relative slopes of fading were also listed as the average values and the order was as follows (Table 1):

$$\text{Violet} > \text{Quinolone} \gg \text{Blue 291} > \text{Yellow 114} > \text{Yellow 211} > \text{Blue 79 : 1} > \text{Blue 165} > \text{Red 73}. \tag{28}$$

If the value of Red 73 is assigned a value of 1.0 as the reference, the relative values of slopes are obtained as listed in Table 1. According to the photo-oxidative model of fading, the slope should be proportional to the product of $k_{0,i}$ and f_i. Dividing the slope by the relative values of $k_{0,i}$, the relative values of f_i were obtained. The order of photosensitivity (the relative values of f_i) for the individual dyes was as follows:

$$\text{Quinolone} > \text{Violet} > \text{Yellow 211} > \text{Blue 291} > \text{Yellow 114} > \text{Blue 79 : 1} > \text{Blue 165} > \text{Red 73}. \tag{29}$$

In the present simple model, the contributions of $k_{0,i}$ and f_i, to photo-oxidative fading should be reflected by their relative values in Table 1.

3.4.3. Analyses of photofading behavior in terms of two parameters

As described in a previous paper [1] and as mentioned above (cf. Section 3.1), the experimental values of $k_{0,\mathrm{Yellow}}/k_{0,\mathrm{Exam}}$ for Quinolone and Yellow 114 were dependent upon the dye combination, whereas the orders deduced for the six

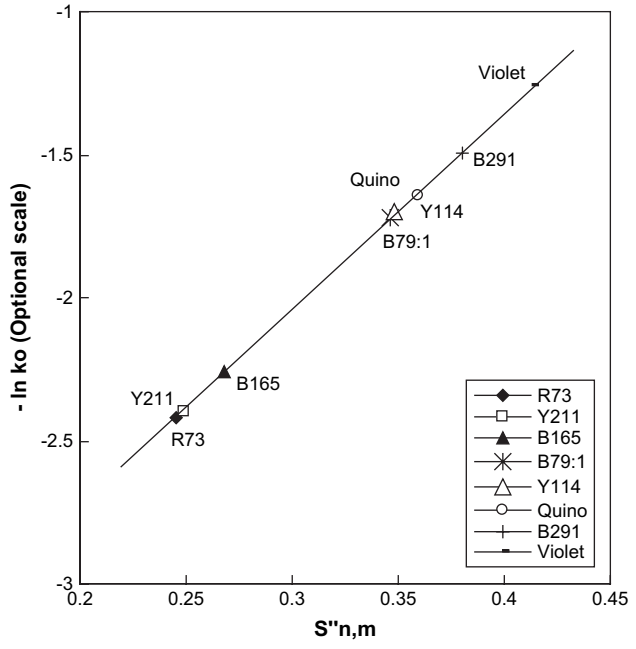

Fig. 1. Relationship between $S''^{(\mathrm{E})}_{m,n}$ and ln k_0 for the disperse azo dyes used. (The name of the dyes is further simplified.)

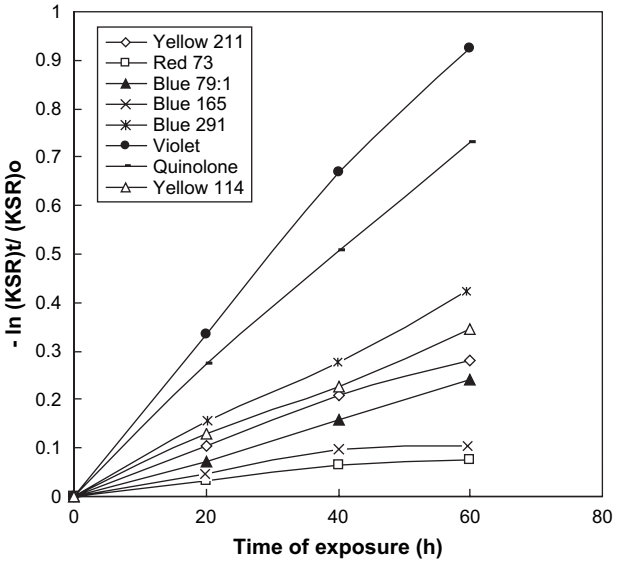

Fig. 2. Rates of fading for disperse azo dyes in the single dyeings of PET fabric upon exposure to a carbon arc in air.

dyes used were almost identical (Tables 3 and 4). Some disagreement between experiments and MO calculation were found in the case of combination dyeings with Yellow 211, the value of which was estimated from the value of $k_{0,Y211}/k_{0,B165}$. No accurate estimation may be possible by the combination dyeing with two yellow dyes, and an indirect estimation was made. The disagreement concerning Yellow 211 may be inevitable. Except for Yellow 211 where an indirect estimation was made, the theoretical (by the MO method) and experimental (by the combination dyeing) estimation for the k_0 values on the whole coincided with each other. Whether or not the $k_{0,i}$ values estimated by the MO method and the f_i values determined experimentally via the $k_{0,i}$ values can explain the results of the $k_{0,Yellow}/k_{0,Exam}$ is the main issue.

From the experimental results, we made the following inferences:

1. The experimental values of $k_{0,Yellow}/k_{0,Exam}$ for the six dyes determined in the combination dyeings with two yellow dyes always gave Quinolone > Yellow 114. In a previous paper [1], the $k_{0,i}$ values for the two dyes were regarded as being large and almost equal to each other. The f_i value for Quinolone was higher than that for Yellow 114, which is one of the obvious experimental results. It can be concluded that the experimental values of $k_{0,Yellow}/k_{0,Exam}$ for each dye examined were strongly influenced by the f_i value.
2. The unsuccessful evaluation of the $k_{0,i}$ value for Yellow 211 (Table 3) implies that no systematic experimental estimation of the $k_{0,i}$ and f_i values for a wide range of dyes was possible using a diagnostic dye. A yellow dye with high $k_{0,i}$ value and low f_i value may be suitable as a diagnostic dye, while a blue dye with the same properties may be suitable as a diagnostic dye for yellow and orange dyes. This was not the case for Blue 165, since Blue 165 had the reverse properties: low $k_{0,i}$ value and high f_i value, indicating that the exceptional experimental $k_{0,Yellow}/k_{0,Exam}$ value for Yellow 211 is natural.
3. The order of the $k_{0,i}$ and f_i values for Blue 165 and Red 73 were similar. But the experimental $k_{0,i}$ value for Red 73 was regarded as being larger than that for Blue 165 (reverse of the theoretical values) by the combination dyeings with both the yellow dyes, while the experimental f_i value for Red 73 was smaller than that for Blue 165. As mentioned above, the $k_{0,Yellow}/k_{0,Exam}$ values obtained for the combination dyeings were dependent upon the f_i values of component dyes, resulting in large $k_{0,Yellow}/k_{0,Exam}$ values determined by Blue 165, which indicated smaller values of $k_{0,B165}$ than the actual values.
4. The addition of two yellow dyes, whose $k_{0,i}$ values were demonstrated above to be almost equal to each other, can elucidate the photochemical properties: the relationship between the initial slope, $k_{0,i}$ and f_i values, LF etc. for eight dyes examined (cf. Table 1). Blue 291, Blue 79:1 and Violet showed high rates of fading, while Red 73, Blue 165 and Yellow 211 possess relatively low rates of fading and low $k_{0,i}$ values. Yellow 211 had high LF irrespective of its high f_i value. Blue 79:1 had intermediate LF in spite of a low f_i value. It is not possible to explain this difference in LF between Yellow 211 and Blue 79:1, although it may be attributable to the lower sensitivity of human vision for yellow hue than for blue hue [1]. Blue 291, Violet, Yellow 114 and Quinolone possess high $k_{0,i}$ values, irrespective of the f_i values. Red 73 and Blue 165 possess both low $k_{0,i}$ and f_i values.

In conclusion, the $k_{0,i}$ values derived using the MO method were supported by the results of our experiments. Thus, the order of (25) or (26) was experimentally demonstrated as being reasonable. These facts including the other dyes describe that the whole fading behavior of disperse dyes examined on PET fabric can be reasonably explained by the present analysis. But whether or not the present procedure to characterize the photofading behavior of disperse dyes can be applied to a whole range of dyes may require further examination.

3.5. Fading on the PET substrate

From the values of ΔE^*_{ab} and ΔL^* listed in Table 2 (for the single dyeing of $N/3$ depth), the six azo dyes examined show fading of the following order:

$$\text{Violet} \gg (\text{Quinolone}) \gg (\text{Yellow 114}) > \text{Yellow 211} > \text{Blue 79 : 1} \approx \text{Blue 291} > \text{Blue 165} > \text{Red 73} \quad (30)$$

The order of Blue 79:1 and Blue 291 was changed, when the results of exposure for 40 and 60 h were taken into consideration. Under these circumstances, these dyes can be regarded as being almost equal in terms of fading.

From the same samples, three types of orders were estimated from the following data:

(1) the rate of fading estimated from the K/S parameters
(2) the ΔE^*_{ab} values of the exposed sample
(3) the LF for the eight disperse azo dyes examined

The order was somewhat different and is listed in Table 1. For example, comparing the order (30) with the LF listed in Table 1, the LF of Yellow 211 was higher, in spite of the higher values of ΔE^*_{ab}, than the LF of Blue 79:1 and Blue 291. This was attributed to differences in the sensitivity of human vision to specific colors as previously explained [1].

Blue 165 seemed to show on-tone fading, i.e., the K/S spectra, which was transformed from the reflectance spectra of the original and exposed samples, showed a steady decrease in K/S values over the full range of wavelengths with time of exposure. The other three dyes, Red 73, Yellow 211 and Yellow 114, exhibited the same pattern in the K/S spectra. Upon exposure, Red 73 showed the lowest value of ΔE^*_{ab} among the dyes examined, while Yellow 114 had a higher ΔE^*_{ab} value. However, a decrease in ΔL^* (indicating an off-tone fading) was observed. In fact, the K/S values at the λ_{max} were decreased with time of exposure, which implied a false indication from the ΔL^* for the reflection spectra.

Table 9
Lightfastness (LF) ratings of disperse azo dyes at various concentrations upon exposure to a carbon arc

	N/50	*N*/12	*N*/6	*N*/3	*N*/2	1/1*N*	2/1*N*
Yellow 211	4–5	4–5	5–6	6–7	(5.14)[a]	7	7
Yellow 114	4–5	4–5	5–6	6	(6.89)[a]	6	6–7
Red 73	3–4	4	No data	5–6 (0.94)[a]		6	6
Blue 165	5	5	5–6	5–6 (1.62)[a]		5–6	6

[a] ΔE^*_{ab} after exposure to a carbon arc for 60 h (cf. Table 2).

Upon exposure, Violet also showed a high rate of on-tone fading, indicating no color change during fading. The fading of Violet was the most extensive, i.e., it showed the lowest LF, among the six dyes. Since this dye had $k_{0,i}$ and f values completely opposite to those of dyes with excellent LF, such as Red 73 and Blue 165, this implied an oxidative mechanism of fading on the PET fabric. The other two dyes, Blue 79:1 and Blue 291, lie between Violet and the three dyes with excellent LF. These two dyes, which have *o*,*p*-dinitro groups show the highest on-tone fading. On the PET substrate, the nitro groups did not exhibit color changes, so these dyes only undergo oxidative fading.

3.6. Concentration dependence of the three parameters

A fundamental problem related to the three above mentioned parameters is concentration dependence, and is summarized in Table 9. Experimentally, the $k_{0,i}$ and f_i values are concentration-dependent. These problems are difficult to overcome theoretically. In general, LF decreases as the dye concentration decreases, in part due to the decline of the filter effect (not aggregation [29]).

The present study describes the mechanism involved in the photofading of disperse dyes on PET. Photochemically the order derived from the *K*/*S* values was useful, while in practice, the order derived from the LF was used. The order obtained from ΔE^*_{ab} should be utilized as mentioned already bearing in mind the various limitations, as it contains many factors that may result in erroneous conclusions [1].

4. Summary

The photofading profiles of six monoazo dyes with a wide range of photochemical properties on PET fabric were analyzed using the Kubelka–Munk parameters from the reflection spectra. Two yellow (pyridone-azo and quinolone-azo) dyes were used in combination dyeings to examine the photo-oxidative properties of the six dyes. The rate constants ($k_{0,i}$) of the reactivity of the azo dyes towards $^1O_2$ were estimated by frontier orbital theory using the PM5 method. The $k_{0,i}$ values derived by the MO method were demonstrated experimentally as being valid.

The photosensitivity values (f_i) of the six dyes on PET were determined from the slope of photofading based on the assumption that the slope of oxidative fading was proportional to the product of $k_{0,i}$ and f_i. The photofading behavior of the dyes on PET can be explained in terms of these two parameters. Dyes that are designed to exhibit superior LF must have low values for both of these parameters.

Acknowledgement

This work was supported by a Grant-in-Aid for Scientific Research from the Ministry of Education, Culture, Sports, Science and Technology, Japan.

References

[1] Okada Y, Hihara T, Morita Z. An analysis of catalytic fading of pyridone azo disperse dyes on polyester substrate using semiempirical molecular orbital PM5 method, Dyes and Pigments, in press.
[2] Hihara T, Okada Y, Morita Z. Azo-hydrazone tautomerism of phenylazonaphthol sulfonates and their analysis using the semiempirical molecular orbital PM5 method. Dyes and Pigments 2003;59(1):25–41.
[3] Hihara T, Okada Y, Morita Z. Reactivity of phenylazonaphthol sulfonates, their estimation by semiempirical molecular orbital PM5 method, and the relation between their reactivity and azo-hydrazone tautomerism. Dyes and Pigments 2003;59(3):201–22.
[4] Hihara T, Okada Y, Morita Z. An analysis of azo-hydrazone tautomerism of reactive azobenzene and pyrazolinylazo dyes, using the semiempirical molecular orbital PM5 method. Dyes and Pigments 2004;61(3):199–225.
[5] Hihara T, Okada Y, Morita Z. Photo-oxidation of pyrazolinylazo dyes and analysis of reactivity as azo and hydrazone tautomers using semiempirical molecular orbital PM5 method. Dyes and Pigments 2006;69(2):151–76.
[6] Hihara T, Okada Y, Morita Z. A semiempirical molecular orbital study on the photo-reactivity of monoazo reactive dyes derived from γ- and J-acids. Dyes and Pigments 2007;73(2):141–61.
[7] Hihara T, Okada Y, Morita Z. Photo-oxidation of reactive azobenzene dyes and an analysis of reactivity as azo and hydrazone tautomers using PM5 method. Dyes and Pigments 2007;75(2):225–45.
[8] Hihara T, Okada Y, Morita Z. An analysis of the photo-reactivity of monoazo reactive dyes derived from H-acid and related naphthalene sulfonic acids using the PM5 method. Dyes and Pigments 2007;75(3):585–605.
[9] Himeno K, Okada Y, Morita Z. Photofading of monoazo disperse dyes on polyester and polyamide substrates. Dyes and Pigments 2000;45(2):109–23.
[10] Stewart JJP. MOPAC 2002 and its manual. Fujitsu Ltd; 2002.
[11] Okada Y, Kato T, Motomura H, Morita Z. Catalytic fading of vinylsulfonyl reactive dye mixtures on cellulose under wet conditions. Dyes and Pigments 1990;12(3):197–211.
[12] Okada Y, Hirose M, Kato T, Motomura H, Morita Z. Fading of vinylsulfonyl reactive dyes on cellulose in admixture under wet conditions. Dyes and Pigments 1990;14(4):265–85.
[13] Leaver AT, Cunningham AD. 17th IFATCC Congress. Vienna: Book of Papers; 5–7 June 1996. p. 59–64.
[14] Rembold MW, Kramer HEA. Singlet oxygen as an intermediate in the catalytic fading of dye mixtures. The Journal of the Society of Dyers and Colourists 1978;94(1):12–7.
[15] Griffiths J, Hawkins C. Mechanistic aspects of the photochemistry of dyes and their intermediates.II – evidence for the formation of singlet oxygen by phototendering vat dyes. The Journal of the Society of Dyers and Colourists 1973;89(2):173–7.
[16] Griffiths J. Solution and polymer photochemistry of azo dyes and related compounds. In: Allen NS, editor. Developments in polymer photochemistry, vol. 1. Essex: Applied Science Publishers Ltd; 1980. p. 145–90 [chapter 6].
[17] Duff DG, Sinclair RS. Giles's laboratory course in dyeing. 4th ed. Bradford: The Society of Dyers and Colourists; 1989.

[18] Vieth WR, Alcalay HH, Frabetti AJ. Solution of gases in oriented poly (ethylene terephthalate). Journal of Applied Polymer Science 1964; 8(5):2125–38.
[19] Fukui K, Fujimoto H. Frontier orbitals and reaction paths. Singapore: World Scientific; 1997.
[20] Fukui K, Yonezawa T, Shingu H. A molecular orbital theory of reactivity in aromatic hydrocarbons. Journal of Chemical Physics 1952;20(4): 722–5.
[21] Fukui K, Yonezawa T, Nagata C, Shingu H. Molecular orbital theory of orientation in aromatic, heteroaromatic and other conjugated molecules. Journal of Chemical Physics 1954;22(8):1433–42.
[22] Fukui K, Yonezawa T, Nagata C. Interrelations of quantum-mechanical quantities concerning chemical reactivity of conjugated molecules. Journal of Chemical Physics 1957;26(4):831–41.
[23] CAChe reference guide, 4.9. Fujitsu Ltd; 2002. p. 3-9–3-10.
[24] Mekenyan O, Peitchev D, Bonchev D, Trinajstić N, Bangov I. Modelling the interactions of small organic molecules with biomacromolecules, I. Interaction of substituted pyridines with anti-3-azopyridine antibody. Arzneimittel-Forschung/Drug Research 1986;36(2):176–83.
[25] Mekenyan O, Bonchev D, Trinajstić N, Peitchev D. Modelling the interactions of small organic molecules biomacromolecules, II. A generalized concept for biological interactions. Arzneimittel-Forschung/Drug Research 1986;36(3):421–4.
[26] Kikuchi O. Systematic QSAR procedures with quantum chemical descriptors. Quantitative Structure–Activity Relationship 1987;6(4): 179–84.
[27] Schüürmann G. QSAR analysis of the acute fish toxicity of organic phosphorothionates using theoretically derived molecular descriptors. Environmental Toxicology and Chemistry 1990;9(4):417–28.
[28] Schüürmann G. Quantitative structure–property relationships for the polarizability, solvatochromic parameters and lipophilicity. Quantitative Structure–Activity Relationships 1990;9(4):326–33.
[29] Hihara T, Okada Y, Morita Z. Photofading, photosensitization, and effect of aggregation on fading of triphenodioxazine and copper phthalocyanine dyes. Dyes and Pigments 2001;50(3):185–201.